

See discussions, stats, and author profiles for this publication at: <https://www.researchgate.net/publication/244461169>

Metal-Free Hydrogen Activation by the Frustrated Lewis Pairs of $\text{ClB}(\text{C}_6\text{F}_5)_2$ and $\text{HB}(\text{C}_6\text{F}_5)_2$ and Bulky Lewis Bases

ARTICLE *in* ORGANOMETALLICS · SEPTEMBER 2009

Impact Factor: 4.13 · DOI: 10.1021/om900517d

CITATIONS

59

READS

38

3 AUTHORS, INCLUDING:



Olivier Blacque

University of Zurich

187 PUBLICATIONS 2,404 CITATIONS

SEE PROFILE



Heinz Berke

University of Zurich

336 PUBLICATIONS 5,721 CITATIONS

SEE PROFILE

Metal-Free Hydrogen Activation by the Frustrated Lewis Pairs of $\text{ClB}(\text{C}_6\text{F}_5)_2$ and $\text{HB}(\text{C}_6\text{F}_5)_2$ and Bulky Lewis Bases

Chunfang Jiang, Olivier Blacque, and Heinz Berke*

Anorganisch-Chemisches Institut, Universität Zürich, Winterthurerstrasse 190, CH-8057 Zürich, Switzerland

Received June 17, 2009

The frustrated Lewis pair (FLP) derived from $\text{ClB}(\text{C}_6\text{F}_5)_2$ and the bulky Lewis bases 2,2,6,6-tetramethylpiperidine (TMP), tri-*tert*-butylphosphine, and tris(2,4,6-trimethylphenyl)phosphine cleaved H_2 heterolytically to form the intermediate anion $[\text{HClB}(\text{C}_6\text{F}_5)_2]^-$, which quickly underwent hydride/chloride exchange with the remaining $\text{ClB}(\text{C}_6\text{F}_5)_2$ to give the known compound $[\text{HB}(\text{C}_6\text{F}_5)_2]_n$ ($n = 1$ or 2) and the anion $[\text{Cl}_2\text{B}(\text{C}_6\text{F}_5)_2]^-$ present in the products $[\text{TMPH}][\text{Cl}_2\text{B}(\text{C}_6\text{F}_5)_2]$ (**1a**), $[t\text{-Bu}_3\text{PH}][\text{Cl}_2\text{B}(\text{C}_6\text{F}_5)_2]$ (**2a**), and $[\text{Mes}_3\text{PH}][\text{Cl}_2\text{B}(\text{C}_6\text{F}_5)_2]$ (**3a**). $[\text{HB}(\text{C}_6\text{F}_5)_2]_n$ forms Lewis adducts with TMP and *t*-Bu₃P: TMP-BH(C_6F_5)₂ (**1b**) and *t*-Bu₃P-BH(C_6F_5)₂ (**2b**). The Lewis adduct *t*-Bu₃P-BH(C_6F_5)₂ was found capable of generating a FLP at elevated temperature and was reacted with H_2 , producing the splitting product $[t\text{-Bu}_3\text{PH}][\text{H}_2\text{B}(\text{C}_6\text{F}_5)_2]$ (**2c**). Mes₃P forms no Lewis adduct with $[\text{HB}(\text{C}_6\text{F}_5)_2]_n$, but a FLP, which was also capable of splitting H_2 to yield initially $[\text{Mes}_3\text{PH}][\text{H}_2\text{B}(\text{C}_6\text{F}_5)_2]$. The $[\text{H}_2\text{B}(\text{C}_6\text{F}_5)_2]^-$ anion underwent disproportionation to form $[\text{Mes}_3\text{PH}][\text{HB}(\text{C}_6\text{F}_5)_3]$ (**3b**), Mes₃P, $[\text{H}_2\text{B}(\text{C}_6\text{F}_5)_2]$, and H_2 . Similarly, 2,4,6-tri-*tert*-butylpyridine (TTBP) and $[\text{HB}(\text{C}_6\text{F}_5)_2]_n$ gave in the presence of H_2 the final products $[\text{TTBPH}][\text{HB}(\text{C}_6\text{F}_5)_3]$ salt and $[\text{H}_2\text{B}(\text{C}_6\text{F}_5)_2]$. The contrasting reactivities of the *t*-Bu₃P/[BH(C_6F_5)₂]_n, Mes₃P/[HB(C_6F_5)₂]_n, and TTBP/[HB(C_6F_5)₂]_n pairs were explained on the basis of the different $\text{p}K_{\text{a}}$'s of the $[\text{LBH}]^+$ cations. After disproportionation of the $[\text{H}_2\text{B}(\text{C}_6\text{F}_5)_2]^-$ anion to give $[\text{Mes}_3\text{PH}][\text{HB}(\text{C}_6\text{F}_5)_3]$ (**3b**) or $[\text{TTBPH}][\text{HB}(\text{C}_6\text{F}_5)_3]$ (**4a**), the also formed $[\text{H}_3\text{B}(\text{C}_6\text{F}_5)]^-$ anion reacted with the more acidic cations $[\text{Mes}_3\text{PH}]^+$, $[\text{TTBPH}]^+$ to give H_2 and *syn*- and *anti*- $[\text{H}_2\text{B}(\text{C}_6\text{F}_5)]_2$ (**3c**). **1a**, **2a**, **3a**, and **4a** were studied by single-crystal X-ray diffraction analysis.

Introduction

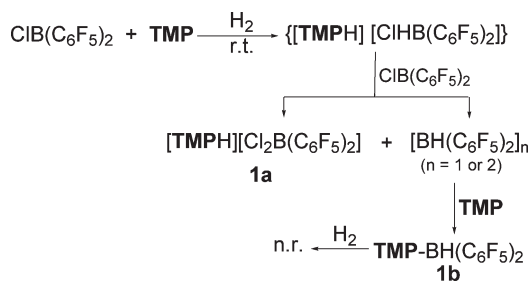
The concept of frustrated Lewis pairs (FLPs) was put forward by D. W. Stephan et al. in 2006 after their remarkable discovery that H_2 can reversibly be activated by the “metal-free” compound $[(2,4,6\text{-C}_6\text{H}_2\text{Me}_3)_2\text{P}(\text{H})(\text{C}_6\text{F}_5)\text{B}(\text{H})(\text{C}_6\text{F}_5)_2]$.¹ As one of the fruitful applications of this concept, “metal-free” catalysts could be developed for the hydrogenation of bulky imines.² In such systems sterically hindered Lewis donors and acceptors are combined to establish encounter complexes. Their steric congestion precludes the formation of classical Lewis adducts, and their relatively close proximity indeed provokes H_2 activation and also “unquenched” reactivity toward small molecules.^{3,4} For instance, the mixtures of frustrated phosphine and borane

pairs can activate H_2 heterolytically under very mild conditions⁵ and can undergo addition of olefins, as well.^{6,7} Similarly following their pioneering work an increasing number of related FLPs were created, which were capable of activating both H_2 heterolytically and also other small molecules.^{8–17} Some of the zwitterionic products resulting from H_2 splitting were shown to serve as active catalysts for the hydrogenation of imines, nitriles, and aziridines, as well as enamine and

*Corresponding author. E-mail: hberke@aci.uzh.ch.

(1) Welch, G. C.; Juan, R. R. S.; Masuda, J. D.; Stephan, D. W. *Science* **2006**, *314*, 1124.(2) Chase, P. A.; Welch, G. C.; Jurca, T.; Stephan, D. W. *Angew. Chem., Int. Ed.* **2007**, *46*, 8050.(3) Stephan, D. W. *Org. Biomol. Chem.* **2008**, *6*, 1535.(4) Stephan, D. W. *Dalton Trans.* **2009**, 3129.(5) Welch, G. C.; Stephan, D. W. *J. Am. Chem. Soc.* **2007**, *129*, 1880.
(6) McCahill, J. S. J.; Welch, G. C.; Stephan, D. W. *Angew. Chem., Int. Ed.* **2007**, *46*, 4968.(7) Ullrich, M.; Seto, K. S.-H.; Lough, A. J.; Stephan, D. W. *Chem. Commun.* **2009**, 2335.(8) Spies, P.; Erker, G.; Kehr, G.; Bergander, K.; Fröhlich, R.; Grimme, S.; Stephan, D. W. *Chem. Commun.* **2007**, 5072.(9) Chase, P. A.; Stephan, D. W. *Angew. Chem., Int. Ed.* **2008**, *47*, 7433.(10) Holschumacher, D.; Bannenberg, T.; Hrib, C. G.; Jones, P. G.; Tamm, M. *Angew. Chem., Int. Ed.* **2008**, *47*, 7428.(11) Sumerin, V.; Schulz, F.; Nieger, M.; Leskelä, M.; Repo, T.; Rieger, B. *Angew. Chem., Int. Ed.* **2008**, *47*, 6001.(12) Huber, D. P.; Kehr, G.; Bergander, K.; Fröhlich, R.; Erker, G.; Tanino, S.; Ohki, Y.; Tatsumi, K. *Organometallics* **2008**, *27*, 5279.(13) Geier, S. J.; Gilbert, T. M.; Stephan, D. W. *J. Am. Chem. Soc.* **2008**, *130*, 12632.(14) Ullrich, M.; Lough, A. J.; Stephan, D. W. *J. Am. Chem. Soc.* **2009**, *131*, 52.(15) Spies, P.; Kehr, G.; Bergander, K.; Wibbeling, B.; Fröhlich, R.; Erker, G. *Dalton Trans.* **2009**, 1534.(16) Ramos, A.; Lough, A. J.; Stephan, D. W. *Chem. Commun.* **2009**, 1118.(17) Geier, S. J.; Stephan, D. W. *J. Am. Chem. Soc.* **2009**, *131*, 3476.(18) Spies, P.; Schwendemann, S.; Lange, S.; Kehr, G.; Fröhlich, R.; Erker, G. *Angew. Chem., Int. Ed.* **2008**, *47*, 7543.

Scheme 1



C=C double bonds of enol silyl ether.^{18–20} Presently FLP formation is no longer limited to boron/phosphine systems, since Stephan et al. and Tamm et al. extended the range of FLPs to boron/carbene combinations, in which for H₂ activation the steric demands of the Lewis pair constituents are very crucial to their reactivity.^{9,10} For the same purpose Rieger et al. introduced the borane/amine variant for FLPs.¹¹ The majority of Lewis acids used were tris(pentafluorophenyl)borane, B(C₆F₅)₃, or closely related molecules. The CIB(C₆F₅)₂ and HB(C₆F₅)₂ compounds were chosen to act as a highly active hydroboration reagents or as synthons for the incorporation of Lewis acidic –B(C₆F₅)₂ groups into molecular frameworks building new intramolecular FLPs.^{8,13,18,19} However, as yet, these compounds have not been used as Lewis acidic components in FLPs to activate H₂. We therefore tried to approach utilization of the “robust” molecules CIB(C₆F₅)₂²¹ and HB(C₆F₅)₂²² in FLPs together with 2,2,6,6-tetramethylpiperidine (TMP) or phosphines R₃P (R = *t*-Bu, 2,4,6-trimethylphenyl = Mes) for cleavage of H₂.

Results and Discussion

Toluene solutions of stoichiometric mixtures of 2,2,6,6-tetramethylpiperidine (TMP) or of the sterically hindered phosphines R₃P (R = *t*-Bu, 2,4,6-trimethylphenyl) and CIB(C₆F₅)₂ were at first explored for Lewis adduct formation by ¹H, ¹⁹F, and ¹¹B NMR spectroscopy. We found only unchanged signals due to the free starting materials and no hint of Lewis adduct formation by these sterically quite congested molecules. We can, however, suppose that contact pairs, the FLPs, had formed, since, for instance, exposure of a TMP/CIB(C₆F₅)₂ toluene solution to an atmosphere of H₂ (1000 mbar) induced a reaction proceeding at ambient temperature. Initial formation of [TMPH][ClHB(C₆F₅)₂] is assumed, but this species is not stable in the presence of CIB(C₆F₅)₂ and is transformed subsequently into the [TMPH][Cl₂B(C₆F₅)₂] salt **1a**. The chloride/hydride metathesis also produces the known equilibrium mixture of the monomeric and dimeric borohydride [HB(C₆F₅)₂]_n (n = 1, 2)²³ (Scheme 1). [HB(C₆F₅)₂]_n quickly associates with the remaining TMP to afford the stable Lewis acid–base adduct TMP-BH(C₆F₅)₂, **1b**. **1b** apparently is such a tight adduct that FLP reactivity toward

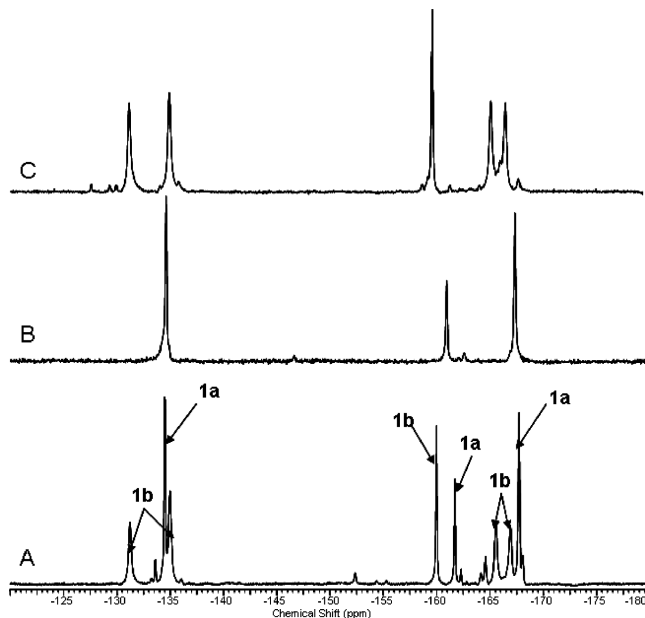


Figure 1. (A) ¹⁹F NMR spectra of the mixture of TMP-CIB(C₆F₅)₂ with H₂ after ca. 30 min in toluene-*d*₈; (B and C) ¹⁹F NMR spectra of pure **1a** and **1b** in toluene-*d*₈.

H₂ could not be initiated even at elevated temperatures (Scheme 1). The formation of **1a** and **1b** according to Scheme 1 could be analyzed by ¹⁹F NMR spectroscopy. The ¹⁹F NMR spectrum of the reaction mixture (spectrum A) and its assignments are shown in Figure 1 in comparison with spectra of pure **1a** (B) and **1b** (C). **1a** could be isolated from the reaction mixture as a white solid in ca. 35% yield. The ¹H NMR spectrum of **1a** features a broad NH₂ resonance at 5.90 ppm, and the ¹⁹F NMR spectrum shows signals at δ –134.56 (*o*-), –160.92 (*p*-), and –167.32 ppm (*m*-C₆F₅), consistent with the four-coordinate boron atom of the anion (Δδ_{m,p} = 3.4). The X-ray diffraction study of **1a** (Figure 2) reveals an overall centrosymmetric chair form of pairs of **1a** held together by hydrogen bonding. Each boron atom is connected to two chlorine atoms and two C₆F₅ groups in a tetrahedral environment.²⁴ The N1–H1 and N1–H2 distances are 0.90(2) and 0.85(2) Å, and the H1–N1–H2 angle is 104.7(2)°. The Cl1–B1–Cl2 angle is 105.42(8)°, and the B–Cl bonds possess an average length of 1.89 Å. Intermolecular N–H···Cl hydrogen bonds link the pairs of ions with H1···Cl1 and H2···Cl2ⁱ separations of 2.50(2) and 2.47(2) Å, respectively.

Pure **1b** was prepared from the reaction of a stoichiometric mixture of [HB(C₆F₅)₂]_n (n = 1 or 2) and TMP obtained as a white solid in 86% yield. In the ¹H NMR spectrum **1b** features a broad H_B resonance at 4.18 ppm, and the ¹¹B NMR resonance is located at δ –11.82 ppm. The ¹⁹F NMR spectrum provides further evidence for the inequivalence of the phenyl rings, since two sets of signals are attributable to the *ortho*- (δ –131.23, –135.06 ppm) and *meta*-fluorine atoms (δ –165.56, –166.92 ppm), but just one signal is found for the *para*-fluorine atoms (δ –160.01 ppm). This

(19) Sumerin, V.; Schulz, F.; Atsumi, M.; Wang, C.; Nieger, M.; Leskelä, M.; Repo, T.; Pykkö, P.; Rieger, B. *J. Am. Chem. Soc.* **2008**, *130*, 14117.

(20) Wang, H.; Fröhlich, R.; Kehr, G.; Erker, G. *Chem. Commun.* **2008**, 5966.

(21) Parks, D. J.; Piers, W. E.; Yap, G. P. A. *Organometallics* **1998**, *17*, 5492.

(22) Parks, D. J.; Spence, R. E. v H.; Piers, W. E. *Angew. Chem., Int. Ed.* **1995**, *34*, 809.

(23) In benzene or toluene solution, bis(pentafluorophenyl)borane exhibits a dimer/monomer equilibrium.

(24) Crystal data for **1a**: C₂₁H₂₀BCl₂F₁₀N₂, *M* = 558.09, monoclinic, *P*2₁/*c*, *a* = 12.0763(2) Å, *b* = 11.2761(2) Å, *c* = 18.3912(3) Å, β = 108.351(2)°, *V* = 2377.04(7) Å³, *Z* = 4, *D*_c = 1.559 g cm^{–3}, μ = 0.362 mm^{–1}, λ = 0.71073 Å, *T* = 183(2) K, 23 392 reflections collected, 4844 independent [*R*_{int}] = 0.0309 and 4150 observed reflections [*I* > 2σ(*I*)], 328 refined parameters, *R* = 0.0298, *wR*₂ = 0.0796. CCDC 736257.

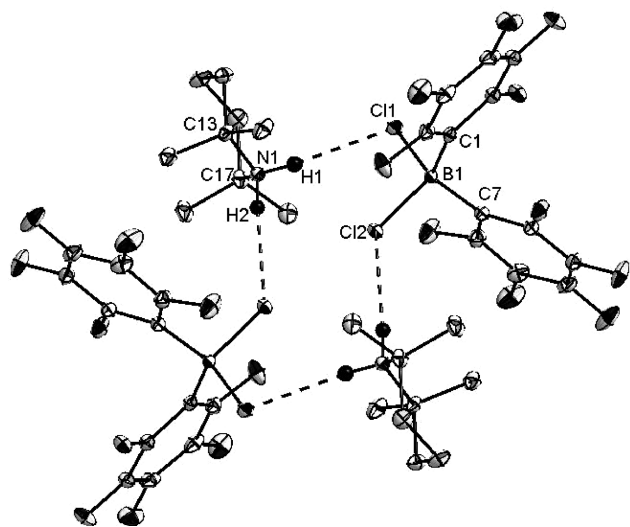
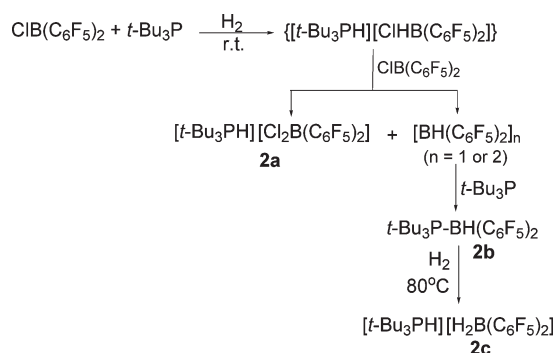


Figure 2. Molecular structure of **1a** with 30% probability thermal ellipsoids. Hydrogen atoms except for the H_N atom are omitted for clarity. Selected bond lengths [Å]: N1–H1 0.90(2), H1...Cl1 2.50(2), N1–H2 0.85(2), H2...Cl2ⁱ 2.47(2), N1–C13 1.532(2), N1–C17 1.529(2), B1–Cl1 1.905(2), B1–Cl2 1.885(2), B1–C1 1.618(2), B1–C7 1.623(2). Selected bond angles [deg]: H1–N1–H2 104.7(2), H1–N1–C17 105.1(1), H1–N1–C13 107.9(1), H2–N1–C13 108.7(1), H2–N1–C17 108.7(1), C13–N1–C17 120.8(1), Cl1–B–Cl2 105.42(8), Cl2–B1–C1 113.89(1), Cl2–B1–C7 104.57(9), C1–B1–C7 115.92(1), Cl1–B1–C7 111.8(1), Cl1–B1–C1 104.95(9), N1–H1...Cl1 174.8(15), N2–H2...Cl2ⁱ 173.6(15). Symmetry transformation (i) used to generate equivalent atoms: 1–*x*, 1–*y*, –*z*.

Scheme 2



observation suggests hindered rotation of the C_6F_5 rings around the B–C bonds, which presumably arises from steric contacts between the methyl substituents of the piperidine moiety and the fluorine atoms or forms $H_{TMP} \cdots F$ hydrogen bonding.

Similar to the reaction with **TMP**, the phosphines $t\text{-Bu}_3\text{P}$ and Mes_3P ($\text{Mes} = 2,4,6\text{-trimethylphenyl}$) were reacted with $\text{ClB}(\text{C}_6\text{F}_5)_2$ under an atmosphere of H_2 to yield initially salts of the phosphonium ions with the unstable $[\text{ClHB}(\text{C}_6\text{F}_5)_2]^-$ anion (Schemes 2 and 3). As for the **TMP** reaction, this anion then undergoes fast hydride/chloride exchange with $\text{ClB}(\text{C}_6\text{F}_5)_2$ to generate the $[\text{Cl}_2\text{B}(\text{C}_6\text{F}_5)_2]^-$ anion and the equilibrium mixture of the monomeric and dimeric hydrides $[\text{HB}(\text{C}_6\text{F}_5)_2]_n$ ($n = 1$ or 2). The products thus were $[\text{t-Bu}_3\text{PH}][\text{Cl}_2\text{B}(\text{C}_6\text{F}_5)_2]$ (**2a**) and $[\text{Mes}_3\text{PH}][\text{Cl}_2\text{B}(\text{C}_6\text{F}_5)_2]$ (**3a**), which exhibit ^{19}F and ^{11}B NMR spectra similar to those resonances

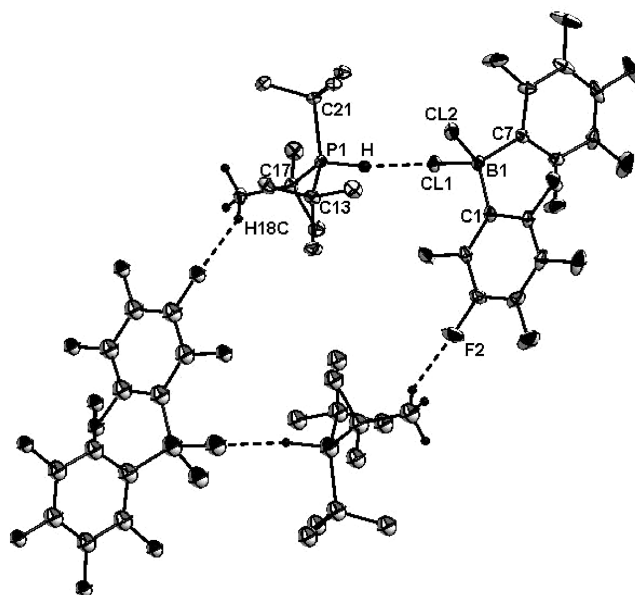


Figure 3. Molecular structure of **2a** with 30% probability thermal ellipsoids. Hydrogen atoms except for the H_P and H_{C18} atoms are omitted for clarity. Selected bond lengths [Å]: P1–H 1.30(2), H...Cl1 2.78(2), H18C...F2ⁱ 2.54, P1–C21 1.869(2), P1–C17 1.867(2), P1–C13 1.871(2), B1–Cl1 1.891(2), B1–Cl2 1.895(2), B1–C1 1.625(2), B1–C7 1.630(2). Selected bond angles [deg]: C21–P1–H 103.7(7), C13–P1–H 104.3(7), C17–P1–H 104.1(6), C21–P–C17 114.72(7), C17–P1–C13 113.95(7), C21–P1–C13 114.26(8), Cl1–B–Cl2 107.64(9), Cl1–B1–C1 113.8(1), Cl1–B1–C7 114.1(1), C1–B1–C7 114.3(1), Cl2–B1–C7 113.28(1), Cl2–B1–C1 103.8(1), P1–H...Cl1 148.1(9), H18C...F2ⁱ 156. Symmetry transformation (i) used to generate equivalent atoms: –*x*, –*y*, 1–*z*.

seen for the $[\text{Cl}_2\text{B}(\text{C}_6\text{F}_5)_2]^-$ anion of **1a**. The cations of **2a** and **3a** show ^{31}P NMR resonances at 51.79 and –25.69 ppm with typically large $J(\text{P},\text{H})$ coupling constants of 440 and 472 Hz, respectively. The ^1H NMR signals of the H_P protons are found at δ 5.12 (**2a**) and 8.48 ppm (**3a**). A crystallographic study of **2a** reveals a square-type structure similar to **1a** (Figure 3). The ions are connected through weak $\text{P}–\text{H} \cdots \text{Cl}$ and $\text{C}–\text{H} \cdots \text{F}$ hydrogen bonds with a $\text{H} \cdots \text{Cl1}$ distance of 2.78(2) and $\text{H18C} \cdots \text{F2A}$ of 2.54 Å.²⁵ The P–H distance is 1.30(2) Å, and the Cl1–B1–Cl2 angle and the Cl–B distance are quite close to those of **1a**. Strong hydrogen bonding could not be traced in the structure of **3a**, and the $\text{Cl2} \cdots \text{H1}$ distance amounts to 2.95 Å, which is significantly longer than the corresponding interactions in **1a** (2.50(2) Å) and **2a** (2.47(2) Å) (Figure 4).²⁶ The Cl1–B1–Cl2 angle and the Cl–B distance of **3a** are comparable to those of **2a**.

The equilibrium mixture of $[\text{HB}(\text{C}_6\text{F}_5)_2]_n$ formed initially according to Schemes 2 and 3 reacted differently with $t\text{-Bu}_3\text{P}$ and Mes_3P . $t\text{-Bu}_3\text{P}$ produced the isolable Lewis adduct

(25) Crystal data for **2a**: $\text{C}_{24}\text{H}_{28}\text{BCl}_2\text{F}_{10}\text{P}$, $M = 619.14$, monoclinic, $P2_1/m$, $a = 8.8527(1)$ Å, $b = 15.7511(2)$ Å, $c = 19.8253(3)$ Å, $\beta = 95.993(2)^\circ$, $V = 2749.33(6)$ Å³, $Z = 4$, $D_c = 1.496$ g cm^{–3}, $\mu = 0.376$ mm^{–1}, $\lambda = 0.71073$ Å, $T = 183(2)$ K, 27971 reflections collected, 6555 independent [$R_{\text{int}} = 0.0455$] and 4858 observed reflections [$I > 2\sigma(I)$], 356 refined parameters, $R = 0.0352$, $wR_2 = 0.0830$. CCDC 736258.

(26) Crystal data for **3a**: $\text{C}_{39}\text{H}_{34}\text{BCl}_2\text{F}_{10}\text{P}$, $M = 805.34$, monoclinic, $P2_1/c$, $a = 8.2098(1)$ Å, $b = 19.2927(2)$ Å, $c = 23.8105(2)$ Å, $\beta = 95.018(1)^\circ$, $V = 3756.87(7)$ Å³, $Z = 4$, $D_c = 1.424$ g cm^{–3}, $\mu = 0.294$ mm^{–1}, $\lambda = 0.71073$ Å, $T = 183(2)$ K, 79873 reflections collected, 11466 independent [$R_{\text{int}} = 0.0331$] and 8553 observed reflections [$I > 2\sigma(I)$], 491 refined parameters, $R = 0.0455$, $wR_2 = 0.1165$. CCDC 736259.

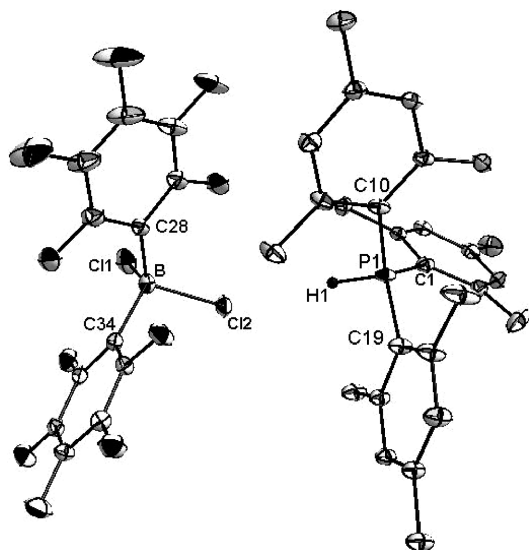


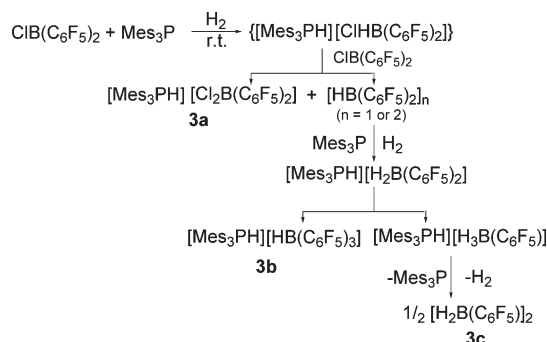
Figure 4. Molecular structure of **3a** with 30% probability thermal ellipsoids. Hydrogen atoms except for the H_P atom are omitted for clarity. Selected bond lengths [Å]: P1–H1 1.30(1), P1–C1 1.80(1), P1–C10 1.80(1), P1–C19 1.81(1), B–Cl1 1.86(2), B–Cl2 1.93(2), B1–C28 1.626(2), B1–C34 1.631(2). Selected bond angles [deg]: C1–P1–C10 114.05(6), C1–P1–C19 115.73(6), C10–P1–C19 115.80(6), C1–P1–H1 103.4(6), C10–P1–H1 102.8(6), C19–P1–H1 102.4(6), Cl1–B–Cl2 107.43(8), Cl2–B–C34 102.99(1), Cl2–B–C28 110.4(1), Cl1–B–C34 114.1(1), Cl1–B–C28 105.9(1), C28–B–C34 115.8(1).

t-Bu₃P–BH(C₆F₅)₂ **2b**. **2b** could independently be prepared from a stoichiometric mixture of [HB(C₆F₅)₂]_n and *t*-Bu₃P in toluene. In the ¹⁹F NMR spectrum it is characterized by a set of signals at δ –124.56 (*o*-), –158.87 (*p*-), and –164.18 ppm (*m*-C₆F₅). The ³¹P NMR signal of this adduct is found at δ 47.64 ppm, and the ¹¹B NMR resonance is at –27.40 ppm, which is consistent with the tetrahedral boron center of **2b**. Interestingly, upon a raise in temperature to 80 °C, **2b** reacted further with H₂, affording the isolable ionic species [*t*-Bu₃PH]–[H₂B(C₆F₅)₂], **2c**. The elevated temperature apparently promotes dissociation of the Lewis adduct to form a FLP.

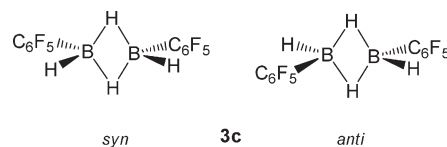
The relative stability of **2c** is mainly attributed to the stability of the anion in the presence of the [*t*-Bu₃PH]⁺ cation, displaying too low acidity²⁷ for further transformation like the salt of this anion with the [Mes₃PH]⁺ cation (*vide infra* Scheme 3). The ¹H and ³¹P NMR spectra of **2c** exhibited the expected resonances. The ¹¹B NMR spectrum shows a triplet at –30.2 ppm with a B–H coupling constant of 90 Hz, and the corresponding ¹H NMR resonance is found at 3.01 ppm (q, br, B–H). Moreover, the Δδ (*m*-F)–(*p*-F) separation is consistent with the presence of an anionic four-coordinate boron atom.

Toluene solutions of stoichiometric mixtures of Mes₃P and [HB(C₆F₅)₂]_n did not lead to formation of a Lewis adduct. The mixture was however found to act as a FLP

Scheme 3



capable of splitting H₂ heterolytically under ambient conditions and generate—somewhat unexpectedly—the [Mes₃PH]–[HB(C₆F₅)₃] salt **3b** as one of the final products. Compound **3b** possesses the following data after exposure of the toluene solution of Mes₃P–[HB(C₆F₅)₂]_n at H₂ atmosphere for 30 min: ¹H NMR δ 7.93 ppm (d, ¹J_{P–H} = 460 Hz); ¹¹B NMR δ –20.21 ppm (d, J_{B–H} = 82 Hz); ¹⁹F NMR δ –133.65, –164.61, –168.34 ppm. Another ¹¹B NMR resonance at 9.5 ppm (br) and a set of ¹⁹F NMR signals at δ –136.79, –137.51, –160.69, –162.14, –166.23, and –166.59 ppm were additionally recognized in the spectra of the reaction solution. These signals were attributed to the *syn* and *anti* isomers of [H₂B(C₆F₅)₂] (3c) formed via disproportionation of the [H₂B(C₆F₅)₂][–] anion.²⁸ But *syn*–[H₂B(C₆F₅)₂] (¹⁹F NMR signals at δ –136.79, –162.14, –166.59 ppm) was not stable in solution and was completely converted after several hours into *anti*–[H₂B(C₆F₅)₂], **3c** (¹⁹F NMR signals at δ –137.51, –160.69, –166.23 ppm). The ¹H NMR spectrum of **3c** was less informative, since resonances for the hydride substituents (terminal or bridging) could not be detected. This was explained on the basis of a broadening of these resonances due to the direct neighborhood with the ¹¹B quadrupole nuclei.



Mes₃P cannot form a stable Mes₃P–BH(C₆F₅)₂ Lewis adduct, but a reactive Mes₃P···BH(C₆F₅)₂ FLP, since reactivity similar to that of the *t*-Bu₃P···BH(C₆F₅)₂ FLP was found. The Mes₃P···BH(C₆F₅)₂ encounter complex can apparently split H₂ to initially generate the [H₂B(C₆F₅)₂][–] anion, which can be detected via ¹¹B NMR as a transient during the reaction process. As a subsequent reaction step, disproportionation of this anion occurs, producing in equilibrium the substituent exchange products [HB(C₆F₅)₃][–] and [H₃B(C₆F₅)][–]²⁹ (Scheme 3). The quite basic [H₃B(C₆F₅)][–] anion is quickly withdrawn from equilibrium via the acid–base reaction with the acidic [Mes₃PH]⁺ cation, evolving H₂

(27) pK_a values, *t*-Bu₃P: 11.4; Ph₃P: 2.73; (*o*-MeC₆H₄)₃P: 3.08; (*p*-MeC₆H₄)₃P: 3.84; TMP: 11.07; TTBP: 4.02. (a) Streuli, C. A. *Anal. Chem.* **1960**, 32, 985. (b) Bush, R. C.; Angelici, R. J. *Inorg. Chem.* **1988**, 27, 681. (c) Cappellani, E. P.; Drouin, S. D.; Jia, G.; Maltby, P. A.; Morris, R. H.; Schweitzer, C. T. *J. Am. Chem. Soc.* **1994**, 116, 3375. (d) Graton, J.; Berthelot, M.; Laurence, C. *J. Chem. Soc., Perkin Trans.* **2001**, 2130. (e) Hall, H. K. *J. Am. Chem. Soc.* **1957**, 79, 5444. (f) Deutsch, E.; Cheung, N. K. *V. J. Org. Chem.* **1973**, 38, 1123.

(28) The monoalkylboranes usually exist as the dimers, and usually the *anti* isomer is thermodynamically more stable than the other. (a) Brown, H. C.; Singaram, B.; Cole, T. E. *J. Am. Chem. Soc.* **1985**, 107, 460. (b) Soundararajan, R.; Matteson, D. S. *Organometallics* **1995**, 14, 4157. (c) Wehmschulte, R. J.; Diaz, A. A.; Khan, M. A. *Organometallics* **2003**, 22, 83.

(29) (a) Biscoe, M. R.; Uyeda, C.; Breslow, R. *Org. Lett.* **2004**, 6, 4331. (b) Biscoe, M. R.; Breslow, R. *J. Am. Chem. Soc.* **2003**, 125, 12718.

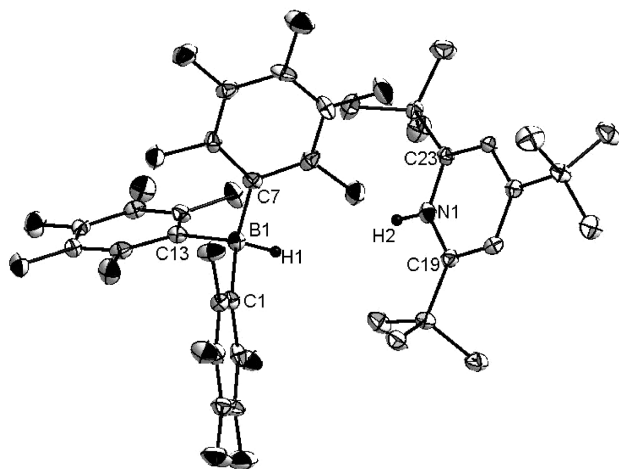
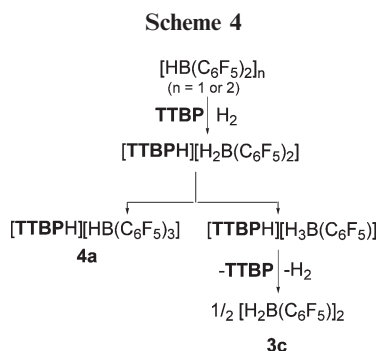


Figure 5. Molecular structure of **4a** with 30% probability thermal ellipsoids. Hydrogen atoms except for the H_N and H_B atoms are omitted for clarity. Selected bond lengths [Å]: B1–H1 1.15(3), B1–C7 1.636(4), B1–C13 1.637(4), B1–C1 1.648(4), N1–H1 0.96(3), N1–C23 1.363(3), N1–C19 1.354(3). Selected bond angles [deg]: C7–B1–H1 107.0(2), C1–B1–H1 103.7(1), C13–B1–H1 108.6(1), C7–B1–C13 112.6(2), C7–B1–C1 114.4(2), C13–B1–C1 110.0(2), H2–N1–C23 115.9(2), H2–N1–C19 119.9(2), C19–N1–C23 124.3 (3).



and forming $[\text{H}_2\text{B}(\text{C}_6\text{F}_5)_2]$ (Scheme 3). It should be mentioned at this point that the $[\text{H}_2\text{B}(\text{C}_6\text{F}_5)_2]^-$ anion of **2c** is also believed to undergo this disproportionation process. The disproportionation occurs for the $[\text{H}_2\text{B}(\text{C}_6\text{F}_5)_2]^-$ anions of both salts $[\text{t-Bu}_3\text{PH}][\text{H}_2\text{B}(\text{C}_6\text{F}_5)_2]$ and $[\text{Mes}_3\text{PH}][\text{H}_2\text{B}(\text{C}_6\text{F}_5)_2]$ (Schemes 2 and 3), however with low actual equilibrium concentrations of the $[\text{H}_3\text{B}(\text{C}_6\text{F}_5)]^-$ anion, too low to enable acid–base reaction with the less acidic $[\text{t-Bu}_3\text{PH}]^+$ cation, but sufficient for the reaction with the more acidic $[\text{Mes}_3\text{PH}]^+$ cation.²⁷

In order to acquire more information about this H_2 splitting reaction with $[\text{HB}(\text{C}_6\text{F}_5)_2]_n$, the bulky Lewis base 2,4,6-tri-*tert*-butylpyridine (TTBP) was applied. TTBP was considered to behave similarly to Mes_3P , since its protonated form possesses a pK_a similar to that of the $[\text{Mes}_3\text{PH}]^+$ cation,²⁷ and in addition the sterically congested TTBP was expected to form a FLP with $[\text{HB}(\text{C}_6\text{F}_5)_2]_n$.

Indeed, the reaction of the $\text{TTBP}/[\text{HB}(\text{C}_6\text{F}_5)_2]_n$ pair with H_2 led to a split of this molecule and also to subsequent disproportionation of the $[\text{TTBPH}][\text{H}_2\text{B}(\text{C}_6\text{F}_5)_2]$ salt to afford the stable $[\text{TTBPH}][\text{HB}(\text{C}_6\text{F}_5)_3]$ compound **4a** and the *syn* and *anti* mixture of **3c** (Scheme 4). **4a** features the same ^1H , ^{11}B , and ^{19}F NMR resonances as the anion of **3b** and also as a compound prepared independently from

$\text{B}(\text{C}_6\text{F}_5)_3$ and TTBP with H_2 . Crystals grown from the crude mixture allowed a X-ray crystallographic study of **4a** (Figure 5), which showed that the B–H and N–H units are oriented toward each other with a $\text{BH} \cdots \text{HN}$ nonbonding distance of 3.51(1) Å, which is much longer than that of other related intermolecular dihydrogen bonding separations.³⁰

In continuation of these investigations, reduction of imines was probed using $\text{HB}(\text{C}_6\text{F}_5)_2$ or $[\text{t-Bu}_3\text{PH}][\text{H}_2\text{B}(\text{C}_6\text{F}_5)_2]$ as catalyst. However, in many cases of the applied imines, the formation of too stable amine–boron adducts prevented the formation of FLPs and consequently also catalytic activity. As a result, only $\text{PhCH}=\text{Nt-Bu}$ could be reduced to the corresponding amine in 95% yield at 120 °C in the presence of 10% $\text{HB}(\text{C}_6\text{F}_5)_2$ at a hydrogen pressure of 1300 mbar within 24 h. For the sterically less hindered imines $\text{PhCH}=\text{NPh}$ and $\text{PhCH}=\text{NCHPh}_2$ the conversions were usually less than 50% under the same conditions as mentioned before. This observation supports the idea that FLP formation is crucial to metal-free hydrogenation catalysis, and anything precluding such a step leads to suppression of catalysis.

Conclusion

In summary, $\text{ClB}(\text{C}_6\text{F}_5)_2$ and $\text{HB}(\text{C}_6\text{F}_5)_2$ were employed as Lewis acids (LAs) in FLP chemistry, and heterolytic splitting of H_2 was observed in the presence of the bulky Lewis bases (LBs) **TMP**, *t-Bu*₃P, Mes_3P , and **TTBP**. The bulkiness of the LB components, the stability of the $[\text{LAH}]^-$ anions toward substituent exchanges, and the acidities of the $[\text{LBH}]^+$ cations were decisive parameters determining the courses of the reactions following the initial H_2 splitting. On the LB side the $[\text{LBH}]^+$ cations $[\text{TMPH}]^+$, $[\text{t-Bu}_3\text{PH}]^+$, $[\text{Mes}_3\text{PH}]^+$, and $[\text{TTBPH}]^+$ were formed and the more acidic ones caused follow-up reactions. On the LA side the initially formed $[\text{LAH}]^-$ anions were subjected to different reaction courses depending on the mentioned parameters. The $[\text{ClHB}(\text{C}_6\text{F}_5)_2]^-$ anions initially formed from $\text{ClB}(\text{C}_6\text{F}_5)_2$ underwent hydride/chloride exchange with $\text{ClB}(\text{C}_6\text{F}_5)_2$ to give $[\text{Cl}_2\text{B}(\text{C}_6\text{F}_5)_2]^-$ and $[\text{HB}(\text{C}_6\text{F}_5)_2]_n$ ($n = 1$ or 2). **TMP** and $[\text{HB}(\text{C}_6\text{F}_5)_2]_n$ ($n = 1$ or 2) formed a tight Lewis adduct, unreactive toward H_2 . At higher temperatures the Lewis adduct *t-Bu*₃P– $\text{BH}(\text{C}_6\text{F}_5)_2$ reacted in the form of its *t-Bu*₃P \cdots $\text{BH}(\text{C}_6\text{F}_5)_2$ FLP with H_2 to generate the salt $[\text{t-Bu}_3\text{PH}][\text{H}_2\text{B}(\text{C}_6\text{F}_5)_2]$. The FLPs $\text{Mes}_3\text{P} \cdots [\text{HB}(\text{C}_6\text{F}_5)_2]$ and $\text{TTBP} \cdots [\text{HB}(\text{C}_6\text{F}_5)_2]$ effected formation of the $[\text{H}_2\text{B}(\text{C}_6\text{F}_5)_2]^-$ anion as a first intermediate, which then underwent disproportionation of the substituents to form $[\text{Mes}_3\text{PH}][\text{HB}(\text{C}_6\text{F}_5)_3]$ or $[\text{TTBPH}][\text{HB}(\text{C}_6\text{F}_5)_3]$ and the quite basic $[\text{H}_3\text{B}(\text{C}_6\text{F}_5)]^-$ anion. Unlike $[\text{t-Bu}_3\text{PH}][\text{H}_2\text{B}(\text{C}_6\text{F}_5)_2]$, where the anticipated equilibrium formation of the $[\text{H}_3\text{B}(\text{C}_6\text{F}_5)]^-$ anion did not lead to a subsequent acid–base reaction with the $[\text{t-Bu}_3\text{PH}]^+$ cation, the $[\text{H}_3\text{B}(\text{C}_6\text{F}_5)]^-$ anion was withdrawn from the disproportionation equilibrium with the more acidic $[\text{Mes}_3\text{PH}]^+$ and $[\text{TTBPH}]^+$ cations, affording H_2 , LB, and *syn*- and *anti*- $[\text{H}_2\text{B}(\text{C}_6\text{F}_5)_2]$.

(30) Crystal data for **4a**: $\text{C}_{38}\text{H}_{38}\text{BF}_{15}\text{N}$, $M = 804.50$, triclinic, $P\bar{1}$, $a = 9.8216(3)$ Å, $b = 10.7921(3)$ Å, $c = 18.7474(6)$ Å, $\alpha = 74.768(3)^\circ$, $\beta = 77.215(3)^\circ$, $\gamma = 78.314(3)^\circ$, $V = 1847.65(10)$ Å³, $Z = 2$, $D_c = 1.446$ g cm^{−3}, $\mu = 0.136$ mm^{−1}, $\lambda = 0.71073$ Å, $T = 183(2)$ K, 19 560 reflections collected, 6995 independent [$R_{\text{int}} = 0.0421$] and 3529 observed reflections [$I > 2\sigma(I)$], 514 refined parameters, $R = 0.0495$, $wR_2 = 0.1148$. CCDC 736260.

Experimental Section

General Considerations. All manipulations were carried out under an atmosphere of dry nitrogen using standard Schlenk techniques or in a glovebox (M. Braun 150B-G-II) filled with dry nitrogen. Solvents were freshly distilled under N_2 by employing standard procedures and were degassed by freeze–thaw cycles prior to use. All organic reagents were purchased from Aldrich and used without further purification. $ClB(C_6F_5)_2$ and $HB(C_6F_5)_2$ were prepared according to the literature.^{21,22} 1H NMR, ^{19}F NMR, $^{11}B\{^1H\}$ NMR, and $^{31}P\{^1H\}$ NMR data were recorded on a Varian Gemini-200 or -300 spectrometer. Chemical shifts are expressed in parts per million (ppm) referenced to the deuterated solvent used. ^{19}F , ^{11}B , and ^{31}P NMR were referenced to $CFCl_3$, $BF_3 \cdot OEt_2$, and 85% H_3PO_4 , respectively. Microanalyses were carried out at the Anorganisch-Chemisches Institut of the University of Zürich.

Crystallographic data were collected at 183(2) K on an Oxford Xcalibur diffractometer (4-circle kappa platform, Ruby CCD detector, and a single-wavelength Enhance X-ray source with Mo $K\alpha$ radiation, $\lambda = 0.71073$ Å).³¹ The selected suitable single crystals were mounted using polybutene oil on the top of a glass fiber fixed on a goniometer head and immediately transferred to the diffractometer. Pre-experiment, data collection, face-indexing analytical absorption correction,³² and data reduction were performed with the Oxford program suite CrysAlisPro.³³ The structures were solved with the direct methods and were refined by full-matrix least-squares methods on F^2 with SHELXL-97.³⁴ All programs used during the crystal structure determination process are included in the WINGX software.³⁵ The program PLATON³⁶ was used to check the results of the X-ray studies and to analyze the hydrogen-bonding systems. The hydrogen atoms bound to nitrogen or phosphorus were located in a difference Fourier map and refined without restraints. All other hydrogen positions were calculated after each cycle of refinement using a riding model with C–H distances in the range 0.93–0.97 Å and their isotropic displacement parameters constrained to $1.2U_{eq}(C)$ or $1.5U_{eq}(C)$.

[TMPH][Cl₂B(C₆F₅)₂], 1a. $ClB(C_6F_5)_2$ (0.076 g, 0.2 mmol) and 2,2,6,6-tetramethylpiperidine (TMP) (0.0283 g, 0.2 mmol) were dissolved in 5 mL of toluene, giving a colorless solution. The reaction vessel was filled with H_2 (1000 mbar), and the solution was stirred at room temperature for 4 h. The reaction mixture was then concentrated to half of its volume, and hexane was added to induce precipitation. The mixture was filtered, washed with hexane, and dried *in vacuo*. **1a** was collected as a white solid. Yield: 35%. Anal. Calcd for $C_{21}H_{20}BCl_2F_{10}N$: C, 45.19; H, 3.61; N, 2.51. Found: C, 45.12; H, 3.63; N, 2.49. 1H NMR (toluene- d_8 , 300 MHz, 293 K): δ 5.90 (br, 2H, N-H), 0.91 ppm (m, overlap, 18H, TMP-CH). $^{11}B\{^1H\}$ NMR (toluene- d_8 , 96 MHz, 293 K): δ -1.68 ppm (br). ^{19}F NMR (toluene, 282 MHz, 293 K): δ -134.56 (d, 4F, $^3J_{F-F} = 25$ Hz, *o*-C₆F₅), -160.92 (t, 2F, $^3J_{F-F} = 20$ Hz, *p*-C₆F₅), -167.32 ppm (t, 4F, $^3J_{F-F} = 23$ Hz, *m*-C₆F₅). $^{13}C\{^1H\}$ NMR (toluene- d_8 , 75 MHz, 293 K): δ 148.32 (dm, $^1J_{C-F} = 258$ Hz, *o*-C₆F₅), 140.51 (dm, $^1J_{C-F} = 263$ Hz, *p*-C₆F₅), 138.15 (dm, $^1J_{C-F} = 262$ Hz, *m*-C₆F₅), 59.17 (*o*-C₅H₇N), 34.37 (*m*-C₅H₇N), 26.93 (CH₃), 15.45 ppm (*p*-C₅H₇N). X-ray quality crystals were obtained from a mixture of toluene/hexane at 25 °C.

TMP-BH(C₆F₅)₂, 1b. $HB(C_6F_5)_2$ (0.0692 g, 0.2 mmol) and 2,2,6,6-tetramethylpiperidine (TMP) (0.0283 g, 0.2 mmol) were dissolved in 2 mL of toluene, and the colorless solution was

stirred at room temperature for 30 min. The solvent was then removed to half of its original volume *in vacuo*. Hexane was added to induce precipitation, and the product was collected as a white solid. Yield: 86%. Anal. Calcd for $C_{21}H_{20}BF_{10}N$: C, 51.77; H, 4.14; N, 2.88. Found: C, 51.69; H, 4.22; N, 2.95. 1H NMR (toluene- d_8 , 300 MHz, 293 K): δ 4.18 (s, 1H, B-H), 1.16 (m, 2H, -CH₂), 0.96 (s, 6H, -CH₃), 0.87 (m, overlap, 4H, -CH₂), 0.82 (s, 6H, -CH₃), 0.73 ppm (s, 1H, N-H). $^{11}B\{^1H\}$ NMR (toluene- d_8 , 96 MHz, 293 K): δ -11.82 ppm (br). ^{19}F NMR (toluene, 282 MHz, 293 K): δ -131.23 (s, 2F, *o*-C₆F₅), -135.06 (s, 2F, *o*-C₆F₅), -160.01 (t, 2F, $^3J_{F-F} = 20$ Hz, *p*-C₆F₅), -165.56 (s, 2F, *m*-C₆F₅), -166.92 ppm (s, 2F, *m*-C₆F₅). $^{13}C\{^1H\}$ NMR (toluene- d_8 , 75 MHz, 293 K): δ 149.61 (dm, $^1J_{C-F} = 245$ Hz, *o*-C₆F₅), 140.50 (dm, $^1J_{C-F} = 242$ Hz, *p*-C₆F₅), 137.93 (dm, $^1J_{C-F} = 241$ Hz, *m*-C₆F₅), 62.03 (*o*-C₅H₇N), 41.82 (*m*-C₅H₇N), 32.33 (CH₃), 16.01 ppm (*p*-C₅H₇N).

[*t*-Bu₃P][Cl₂B(C₆F₅)₂], 2a. $ClB(C_6F_5)_2$ (0.076 g, 0.2 mmol) and tri-*tert*-butylphosphine (0.0405 g, 0.2 mmol) were dissolved in 5 mL of toluene, giving a yellow solution. The reaction vessel was filled with H_2 (1000 mbar), and the solution was stirred at room temperature for 2 h. Some precipitate had formed during the process. The reaction mixture was concentrated to half of its original volume, and hexane was added to induce precipitation. The mixture was filtered, washed with hexane, and dried *in vacuo*. **2a** was collected as a white solid. Yield: 47%. Anal. Calcd for $C_{24}H_{28}BCl_2F_{10}P$: C, 46.56; H, 4.56. Found: C, 46.48; H, 4.71. 1H NMR ($CDCl_3$, 200 MHz, 293 K): δ 5.12 (d, 1H, $^1J_{H-P} = 440$ Hz, P-H), 1.70 ppm (d, 27H, $^3J_{H-P} = 16$ Hz, P{C(CH₃)₃}). $^{11}B\{^1H\}$ NMR ($CDCl_3$, 64 MHz, 293 K): δ -4.50 ppm (br). $^{31}P\{^1H\}$ NMR ($CDCl_3$, 81 MHz, 293 K): δ 51.79 ppm (s). ^{19}F NMR ($CDCl_3$, 188 MHz, 293 K): δ -134.09 (dd, 4F, $^3J_{FF} = 23$ Hz, $^4J_{F-Cl} = 7$ Hz, *o*-C₆F₅), -161.61 (t, 2F, $^3J_{FF} = 23$ Hz, *p*-C₆F₅), -166.80 ppm (td, 4F, $^3J_{FF} = 23$ Hz, $^5J_{F-Cl} = 7$ Hz, *m*-C₆F₅). $^{13}C\{^1H\}$ NMR ($CDCl_3$, 50 MHz, 293 K): δ 147.32 (dm, $^1J_{C-F} = 242$ Hz, *o*-C₆F₅), 139.21 (dm, $^1J_{C-F} = 247$ Hz, *p*-C₆F₅), 136.9 (dm, $^1J_{C-F} = 247$ Hz, *m*-C₆F₅), 37.38 (d, $^1J_{C-P} = 28$ Hz, P{C(CH₃)₃}), 30.04 ppm (s, P{C(CH₃)₃}). X-ray quality crystals were obtained from a mixture of toluene/hexane at 25 °C.

***t*-Bu₃P-BH(C₆F₅)₂, 2b.** In a NMR tube a suspension of $HB(C_6F_5)_2$ (0.0346 g, 0.1 mmol) in toluene- d_8 (0.5 mL) was prepared. Tri-*tert*-butylphosphine (0.02 g, 0.1 mmol) was then added to the suspension. The tube was capped with a rubber septum, and the suspension was vigorously shaken until all solid had dissolved (approximately 5 min). Anal. Calcd for $C_{24}H_{28}BF_{10}P$: C, 52.58; H, 5.15. Found: C, 52.50; H, 5.14. 1H NMR (toluene- d_8 , 200 MHz, 293 K): δ 4.20 (br, 1H, B-H), 1.11 ppm (d, 27H, $^3J_{H-P} = 12$ Hz, P{C(CH₃)₃}). $^{11}B\{^1H\}$ NMR (toluene- d_8 , 64 MHz, 293 K): δ -27.40 ppm (br). $^{31}P\{^1H\}$ NMR (toluene- d_8 , 81 MHz, 293 K): δ 47.64 ppm (br). ^{19}F NMR (toluene- d_8 , 188 MHz, 293 K): δ -124.56 (br, 4F, *o*-C₆F₅), -158.87 (t, 2F, $^3J_{F-F} = 21$ Hz, *p*-C₆F₅), -164.18 ppm (br, 4F, *m*-C₆F₅). $^{13}C\{^1H\}$ NMR (toluene- d_8 , 50 MHz, 293 K): δ 148.54 (dm, $^1J_{C-F} = 242$ Hz, *o*-C₆F₅), 140.28 (dm, $^1J_{C-F} = 223$ Hz, *p*-C₆F₅), 137.96 (dm, $^1J_{C-F} = 242$ Hz, *m*-C₆F₅), 39.55 (d, $^1J_{C-P} = 18$ Hz, P{C(CH₃)₃}), 31.14 ppm (s, P{C(CH₃)₃}).

[*t*-Bu₃P][H₂B(C₆F₅)₂], 2c. $HB(C_6F_5)_2$ (0.0692 g, 0.2 mmol) and tri-*tert*-butylphosphine (0.0405 g, 0.2 mmol) were dissolved in 5 mL of toluene, giving a slurry. The reaction vessel was filled with H_2 (1000 mbar), and the solution was stirred at 80 °C for 24 h. The reaction mixture was then concentrated to half of its original volume, and hexane was added to induce precipitation. The mixture was filtered, washed with hexane, and dried *in vacuo*. The product was collected as a white solid. Yield: 78%. Anal. Calcd for $C_{24}H_{30}BF_{10}P$: C, 52.39; H, 5.50. Found: C, 52.27; H, 5.41. 1H NMR ($CDCl_3$, 200 MHz, 293 K): δ 5.12 (d, 1H, $^1J_{H-P} = 450$ Hz, P-H), 3.01 (q, br, 1H, $^1J_{H-B} = 90$ Hz, B-H), 1.70 ppm (d, 27H, $^3J_{H-P} = 16$ Hz, P{C(CH₃)₃}). $^{11}B\{^1H\}$ NMR ($CDCl_3$, 64 MHz, 293 K): δ -30.20 ppm (s). $^{31}P\{^1H\}$ NMR ($CDCl_3$, 81 MHz, 293 K): δ 53.88 ppm (s). ^{19}F NMR ($CDCl_3$,

(31) Xcalibur CCD System; Oxford Diffraction Ltd: Abingdon, Oxfordshire, England, 2007.

(32) Clark, R. C.; Reid, J. S. *Acta Crystallogr.* **1995**, *A51*, 887–897.

(33) CrysAlisPro (Versions 1.171.32/33); Oxford Diffraction Ltd: Abingdon, Oxfordshire, England.

(34) Sheldrick, G. M. *Acta Crystallogr.* **2008**, *A64*, 112–122.

(35) Farrugia, L. J. *J. Appl. Crystallogr.* **1999**, *32*, 837.

(36) Spek, A. L. *J. Appl. Crystallogr.* **2003**, *36*, 7–13.

188 MHz, 293 K): δ -134.09 (d, 4F, $^3J_{\text{FF}} = 20$ Hz, *o*-C₆F₅), -165.85 (t, 2F, $^3J_{\text{FF}} = 21$ Hz, *p*-C₆F₅), -167.97 ppm (t, 4F, $^3J_{\text{FF}} = 20$ Hz, *m*-C₆F₅). $^{13}\text{C}\{^1\text{H}\}$ NMR (CDCl₃, 50 MHz, 293 K): δ 147.48 (dm, $^1J_{\text{C-F}} = 243$ Hz, *o*-C₆F₅), 139.65 (dm, $^1J_{\text{C-F}} = 244$ Hz, *p*-C₆F₅), 136.36 (dm, $^1J_{\text{C-F}} = 247$ Hz, *m*-C₆F₅), 36.88 (d, $^1J_{\text{C-P}} = 28$ Hz, P{C(CH₃)₃}), 30.15 ppm (s, P{C(CH₃)₃}).

[Mes₃PH][Cl₂B(C₆F₅)₂], 3a. ClB(C₆F₅)₂ (0.0380 g, 0.1 mmol) and trimesitylphosphine (0.0388 g, 0.1 mmol) were dissolved in 2 mL of toluene, giving a pink solution. The reaction vessel was filled with H₂ (1000 mbar), and the solution was stirred at room temperature for 2 h. The reaction mixture was then concentrated to half of its original volume, and hexane was added to induce precipitation. The mixture was filtered, washed with hexane, and dried *in vacuo*. **3a** was collected as a white solid. Yield: 30%. Anal. Calcd for C₃₉H₃₄BCl₂F₁₀P: C, 58.16; H, 4.26. Found: C, 58.08; H, 4.20. ^1H NMR (toluene-*d*₈, 200 MHz, 293 K): δ 8.48 (d, 1H, $^1J_{\text{H-P}} = 472$ Hz, P-H), 6.52 (s, 6H, P(C₆H₂)₃), 2.16 (s, 9H, P(C₆H₂Me-4)), 1.95 (s, 9H, P(C₆H₂Me-2)), 1.65 ppm (s, 9H, P(C₆H₂Me-6)). $^{11}\text{B}\{^1\text{H}\}$ NMR (toluene-*d*₈, 64 MHz, 293 K): δ -4.72 ppm (br). $^{31}\text{P}\{^1\text{H}\}$ NMR (toluene-*d*₈, 81 MHz, 293 K): δ -25.69 ppm (s). ^{19}F NMR (toluene-*d*₈, 188 MHz, 293 K): δ -132.51 (d, 4F, $^3J_{\text{F-F}} = 24$ Hz, *o*-C₆F₅), -162.46 (t, 2F, $^3J_{\text{F-F}} = 21$ Hz, *p*-C₆F₅), -167.08 ppm (t, 4F, $^3J_{\text{F-F}} = 21$ Hz, *m*-C₆F₅). $^{13}\text{C}\{^1\text{H}\}$ NMR (toluene-*d*₈, 50 MHz, 293 K): δ 148.32 (dm, $^1J_{\text{C-F}} = 242$ Hz, *o*-C₆F₅), 146.42 (*para*-C₆H₂), 143.87 (*ortho*-C₆H₂), 139.95 (dm, $^1J_{\text{C-F}} = 247$ Hz, *p*-C₆F₅), 137.23 (dm, $^1J_{\text{C-F}} = 247$ Hz, *m*-C₆F₅), 132.49 (*meta*-C₆H₂), 112.28 (d, $^1J_{\text{C-P}} = 81$ Hz, P-C₆H₂), 21.79 (C₆H₂Me-6), 21.56 (C₆H₂Me-4), 19.25 ppm (C₆H₂Me-2). X-ray quality crystals were obtained from toluene/hexane solution at 25 °C.

[Mes₃PH][HB(C₆F₅)₃], 3b. HB(C₆F₅)₂ (0.0692 g, 0.2 mmol) and trimesitylphosphine (0.0776 g, 0.2 mmol) dissolved in 5 mL of toluene, giving a slurry solution. The reaction vessel was filled with H₂ (1000 mbar), and the reaction mixture was stirred at room temperature for 8 h. The reaction mixture was concentrated to half of its original volume, and hexane was added to induce precipitation. The mixture was filtered, washed with hexane, and dried *in vacuo*. The product was collected as a white solid. Yield: 56%. Anal. Calcd for C₄₅H₃₅BF₁₅P: C, 59.89; H, 3.91. Found: C, 59.67; H, 3.61. ^1H NMR (CDCl₃, 200 MHz, 293 K): δ 8.06 (d, 1H, $^1J_{\text{H-P}} = 456$ Hz, P-H), 7.12 (d, 6H, $^4J_{\text{H-P}} = 12$ Hz, P(C₆H₂)₃), 2.37 (s, 9H, P(C₆H₂Me-4)), 2.27 (s, 9H, P(C₆H₂Me-2)), 1.99 ppm (s, 9H, P(C₆H₂Me-6)). $^{11}\text{B}\{^1\text{H}\}$ NMR (CDCl₃, 64 MHz, 293 K): δ -25.63 ppm (s). $^{31}\text{P}\{^1\text{H}\}$ NMR (CDCl₃, 81 MHz, 293 K): δ -26.95 ppm (s). ^{19}F NMR (CDCl₃, 188 MHz, 293 K): δ -134.64 (d, 6F, $^3J_{\text{FF}} = 21$ Hz,

o-C₆F₅), -165.74 (t, 3F, $^3J_{\text{FF}} = 21$ Hz, *p*-C₆F₅), -168.52 ppm (t, 6F, $^3J_{\text{FF}} = 24$ Hz, *m*-C₆F₅).

[H₂B(C₆F₅)₂], 3c. There was no evidence for signals of the bridging or terminal hydrides in the ^1H NMR spectrum. ^{19}F NMR (toluene-*d*₈, 282 MHz, 293 K): *syn*-[H₂B(C₆F₅)₂] δ -136.79 (d, $^3J_{\text{F-F}} = 20$ Hz, *o*-C₆F₅), -162.14 (t, $^3J_{\text{F-F}} = 21$ Hz, *p*-C₆F₅), -166.59 ppm (t, $^3J_{\text{F-F}} = 20$ Hz, *m*-C₆F₅). *anti*-[H₂B(C₆F₅)₂] δ -137.51 (d, $^3J_{\text{FF}} = 21$ Hz, *o*-C₆F₅), -160.69 (t, $^3J_{\text{FF}} = 21$ Hz, *p*-C₆F₅), -166.23 ppm (t, $^3J_{\text{FF}} = 20$ Hz, *m*-C₆F₅). ^{11}B NMR (toluene-*d*₈, 96 MHz, 293 K): δ 9.5 ppm (br).

[TTBPH][HB(C₆F₅)₃], 4a. HB(C₆F₅)₂ (0.0692 g, 0.2 mmol) and 2,4,6-tri-*tert*-butylpyridine (0.05 g, 0.2 mmol) were dissolved in 5 mL of toluene, giving a slurry. The reaction vessel was filled with H₂ (1000 mbar). The solution was stirred at 120 °C for 24 h, during which time a white precipitate formed. The reaction mixture was concentrated to half of its original volume, and hexane was added to induce complete precipitation. The mixture was filtered, washed with hexane, and dried *in vacuo*. The product was collected as a white solid. Yield: 38%. Anal. Calcd for C₃₅H₃₁BF₁₅N: C, 55.21; H, 4.10; N, 1.84. Found: C, 55.60; H, 4.18; N, 1.87. ^1H NMR (CDCl₃, 200 MHz, 293 K): δ 10.66 (br, 1H, N-H), 7.72 (s, 2H, Ar-H), 3.40 (q, br, 1H, $^1J_{\text{H-B}} = 86$ Hz, B-H), 1.49 (s, 18H, *t*-Bu), 1.40 ppm (s, 9H, *t*-Bu). ^{19}F NMR (CDCl₃, 188 MHz, 293 K): δ -134.69 (d, 6F, $^3J_{\text{F-F}} = 21$ Hz, *o*-C₆F₅), -165.41 (t, 3F, $^3J_{\text{F-F}} = 21$ Hz, *p*-C₆F₅), -168.43 ppm (t, 6F, $^3J_{\text{F-F}} = 21$ Hz, *m*-C₆F₅). $^{11}\text{B}\{^1\text{H}\}$ NMR (CDCl₃, 64 MHz, 293 K): δ -30.73 ppm (s). $^{13}\text{C}\{^1\text{H}\}$ NMR (CDCl₃, 50 MHz, 293 K): δ 163.69 (*o*-C₅H₂N), 150.95 (*p*-C₅H₂N), 147.84 (dm, $^1J_{\text{C-F}} = 238$ Hz, *o*-C₆F₅), 139.27 (dm, $^1J_{\text{C-F}} = 240$ Hz, *p*-C₆F₅), 136.00 (dm, $^1J_{\text{C-F}} = 243$ Hz, *m*-C₆F₅), 120.66 (*m*-C₅H₂N), 37.88 (*o*-C(CH₃)), 37.67 (*p*-C(CH₃)), 30.16 (*p*-C(CH₃)), 28.98 (*o*-C(CH₃)). X-ray quality crystals were obtained from a toluene/hexane solution at 25 °C.

[H₂B(C₆F₅)₂], 3c. ^{19}F NMR (toluene-*d*₈, 282 MHz, 293 K): *syn*-[H₂B(C₆F₅)₂] δ -137.08 (*o*-C₆F₅), -161.85 (*p*-C₆F₅), -166.65 ppm (*m*-C₆F₅); *anti*-[H₂B(C₆F₅)₂] δ -137.70 (*o*-C₆F₅), -161.06 (*p*-C₆F₅), -166.32 ppm (t, $^3J_{\text{F-F}} = 20$ Hz, *m*-C₆F₅). ^{11}B NMR (toluene-*d*₈, 96 MHz, 293 K): δ 8.2 ppm (br).

Acknowledgment. Support from the Swiss National Science Foundation and the Funds of the University of Zurich are gratefully acknowledged.

Supporting Information Available: CIF files giving details of the X-ray crystal structure analysis (**1a**, **2a**, **3a**, **4a**). This material is available free of charge via the Internet at <http://pubs.acs.org>.